JOURNAL OF CATALYSIS 99, 316–326 (1986)

Preparation and Characterization of Pillared Hectorite Catalysts

MARIO L. OCCELLI*,[1] AND DENNIS H. FINSETH†

*Gulf Research & Development Company, P.O. Drawer 2038; and †Department of Energy, Pittsburgh Energy Technology Center, P.O. Box 10940, Pittsburgh, Pennsylvania 15230

Received June 28, 1985; revised January 3, 1986

Reaction of natural hectorite with Al, ZrAl, and Zr polyoxycations generate pillared hectorites which after heating in air at 400°C/4 h have Langmuir surface areas of 260–300 m^2/g thermally stable to 600–700°C. Spectroscopic studies of sorbed pyridine indicate that these pillared hectorites (like pillared bentonites) contain both Lewis and Brønsted acid sites distributed as in the parent (acid-washed) hectorite. Above 300°C, *in vacuo*, pyridine is sorbed mainly on Lewis sites. Pillared hectorites are not as active as the corresponding pillared bentonites in cracking 260–426°C boiling range gas oils but exhibit greater gasoline selectivity and minimize light gases (C_2–C_4) generation. Cracking activity depends mostly on the surface area generated by pillaring and the parent hectorite low iron content did not affect the catalyst's carbon selectivity.

INTRODUCTION

Because pillared clays could be used in conventional petrochemical processes (such as fluid catalytic cracking and hydrotreating), these materials have been receiving a great deal of attention from the petroleum engineer. This new class of catalysts has been reviewed recently by Pinnavaia (*1*). Of particular interest are the properties of clays pillared with oxide clusters since these microporous structures have the high thermal stability necessary in most petrochemical applications. Only pillared montmorrillonites have been reported to have useful cracking activity in such important applications as gas oil cracking, the major process for gasoline production (*2*). However, hydrothermal stability (necessary for catalyst regeneration) will have to be improved before commercial use in fluid cracking applications can occur (*3*).

Pillaring of hectorite with heat-stable inorganic oxide clusters has been accomplished by Endo *et al.* (*4*) by hydrolyzing a silicon acetylacetonate complex in the interlamellar region of the mineral. Shabtai *et al.* (*5*) reported that by reacting La^{3+}- and Ce^{3+}-exchanged hectorites with oligomeric hydroxyaluminum cations, pillared materials stable to 500°C are obtained. Recently Pinnavaia and his co-workers (*6*) discovered that the same hydroxyaluminum oligomer used in pillaring montmorillonites and hectorites can be used to delaminate clays. A delaminated (DL) synthetic hectorite was found to have: (1) gasoline selectivity (in cracking gas oil) similar to commercial fluid cracking catalysts containing zeolites; and (2) light cycle gas oil (LCGO used as furnace oil) selectivity typical of pillared clays (*7*). Both clay catalysts have limited hydrothermal stability.

This paper explores the properties of hectorite pillared with Al_2O_3, ZrO_2–Al_2O_3, and ZrO_2 clusters and presents the physicochemical and cracking activity of these novel materials.

EXPERIMENTAL

Surface Properties

A DIGISORB 2600 from Micromeritics Instrument Corporation was used to measure N_2 sorption, Langmuir and BET surface area, and pore size distributions. Mercury penetration porosimetry measurements were performed using a

[1] Present address: Union Oil Co. of California, Science and Technology Division, P.O. Box 76, Brea, Calif. 92621.

0021-9517/86 $3.00

Quantachrome porosimeter. Differential thermal analysis (DTA) and thermal gravimetric analysis (TGA) were obtained with a DuPont 1090 thermogravimetric analyzer using heating rates of 20 and 10°C/min, respectively. Air (50 cm^3/min) was used as a purge gas; the sample weight was ~35 mg. Infrared spectra (IR) were obtained with a Perkin–Elmer PE-180 spectrometer. Self-supporting wafers were prepared by pressing 15-mg samples on a 13-mm-diameter die for 1 min at ~8000 lb under vacuum. Prior to pyridine sorption, the wafers were mounted in an optical cell and degassed by heating at 300°C for 10 h at 10^{-6} Torr. The pyridine-loaded wafers were then heated (*in vacuo*) in the 200–500°C temperature range (at 100°C intervals) for periods of 1 h and the spectra recorded for each temperature. X-Ray powder patterns were recorded using a Rigaku computer-controlled diffractometer equipped with a receiving graphite monochromator to obtain monochromatic Cu$K\alpha$ radiation and a scintillation detector.

Pillared Hectorites Preparation

ACH-Hectorite. The natural hectorite used was supplied in spray-dried form by the Industrial Chemicals Division of NL Industries. It contained calcite and dolomite impurities and had BET surface area of ~75 m^2/g; chemical composition is shown in Table 1. The pH of a slurry, formed by adding 50 g of clay to 10 liters distilled water, was reduced to 4.3 with 20% HCl. An excess (150 g) of aluminum chlorohydroxide (ACH) solution (chlorhydrol from the Reheis Chemical Co.) was added dropwise and the slurry stirred vigorously for 1 h at 50°C. After filtration (under vacuum) and washing with 6 liters of hot (50°C) distilled water, the wet cake was reslurried in 10 liters of distilled water and stirred for 1 h. The slurry was again filtered and the pillared hectorite washed and air-dried to a consistency which allowed forming into 1/16-in. extrudates with a bench-scale 2-in. Bonnot extruder. The air-dried extrudates could then be crushed with ease and sized into 100 × 325 mesh granules for evaluation and catalytic testing.

ZCH-Hectorite. Aqueous zirconyl chloride (ZCH) was prepared by diluting 483 g of 20% $ZrOCl_2$ solution (from Magnesium Elektron, Inc.) to 3 liters with distilled water and then by aging at 60°C for 48 h. This solution was added (dropwise) to a slurry containing 50 g hectorite in 10 liters distilled water titrated to pH 4.0 with 20% HCl; the final pH of the slurry was 1.9. After stirring for 0.5 h at 20°C, the pillared clay was washed by twice repeating the washing steps described above in preparing ACH-hectorite. The wet clay was formed into 1/

TABLE 1

Chemical Analysis before and after Pillaring (wt% on Dry Basis)[a]

	Hectorite	ACH-Hectorite	ZACH-Hectorite	ZCH-Hectorite	DL-Hectorite
SiO_2	58.20	55.30	55.06	47.73	51.15
Al_2O_3	0.97	14.50	8.76	0.73	21.02
MgO	26.25	23.30	22.25	18.98	24.08
CaO	4.87	0.10	0.05	0.05	0.04
Na_2O	2.62	0.28	0.24	0.17	0.14
K_2O	0.22	0.17	0.12	0.09	0.06
Li_2O	0.51	0.50	0.48	0.48	0.29
Fe_2O_3	0.26	0.28	0.29	0.22	0.07
ZrO_2	—	—	8.37	26.80	—
	93.39	93.93	95.62	95.25	96.85

[a] The difference from 100 is due to residual H_2O.

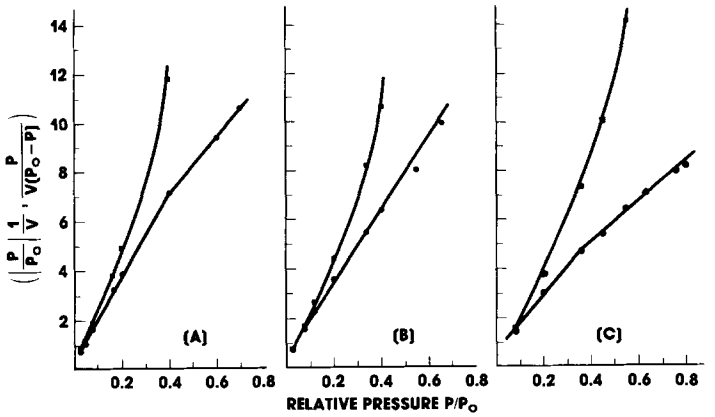

FIG. 1. Nitrogen sorption isotherms for: (A) ACH-, (B) ZACH-, and (C) ZCH-hectorite after drying at 400°C/4 h in air.

16-in. extrudates, air-dried, and crushed to the desired size.

ZACH-Hectorite. This pillared clay was prepared using the procedure employed in forming ACH-hectorite. The interlayering cation was prepared by diluting 73 g of REZAL 67 (Reheis) to 2 liters with distilled water and by aging the solution for 48 h at 60°C.

Reheis REZAL-67 is a solution, thought to contain randomly polymerized polynuclear cations with an approximate Al/Zr ratio of 6.7; the metals/Cl ratio is ~1.0. These solutions are stable to pH values up to 4.0 whereas zirconium chlorhydrate salts precipitate at pH values between 2.0 and 2.5. Synthesis of a Zr, Al chlorhydrated (ZACH) complex with the empirical formula $[ZrOCl_2 \cdot Al_8(OH)_{20}]^{4+}$ has been described by Beckman (*8*).

Synthesis and characterization of the delaminated (DL) hectorite catalyst used in this work has been described in detail in the literature (*6, 7*).

Cracking Activity

The catalyst's cracking activity was evaluated with a flow system similar to that described by Ciapetta and Henderson (*9*). Feedstock was a gas oil (260–426°C boiling range) containing 23.0 wt% furnace oil (221–343°C) and 74.3 wt% slurry oil (343–426°C). The charge consisted of 2.5 g of 100 × 325 mesh granules calcined in dry air in the 300–800°C temperature range. Typical test conditions were: 515°C reactor temperature, 80-s contact time, and 15 WHSV. Percentage conversion is defined as: $(V_f - V_p)\ 100/V_f$ where V_f is the volume of fresh feed (FF) cracked and V_p is the volume of product boiling above 204°C.

RESULTS AND DISCUSSION

Surface Area and Stability

As previously reported, the Langmuir equation best represents nitrogen as well as nC_5–nC_{10} sorption isotherms in bentonites pillared with ZrO_2 and Al_2O_3 clusters since multimolecular sorption in these clays is limited by pillar height (*10–12*). Figure 1 shows that similar results are obtained with pillared hectorites (*5*). In all cases, the BET equation gives curves concave upward and only the Langmuir equation gives straight lines for P/P_0 values between 0.05 and 0.80. The change in slope in Fig. 1 is attributed to a variation in the isosteric heat of sorption due to variable microporosity resulting from inhomogeneities in pillars distribution and in clay platelets stacking. Similar isotherms have been reported for the sorption of *n*-hexane and benzene in mordenite (*13*); this zeolite has two volumes available for sorption characterized by (elliptical) open-

TABLE 2

Pillared Hectorites Thermal Stability
(4 h at Temperature in Air)

Calcination temperature (°C)	% Retention surface area		
	ACH	ZACH	ZCH
300	100.0	100.0	100.0
400	99.0	91.0	95.4
500	95.0	91.0	96.4
600	81.0	89.5	95.3
700	44.7	44.2	77.0

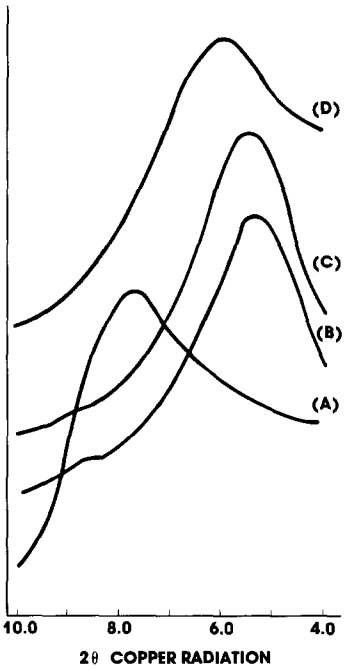

FIG. 2. X-Ray diffractograms of hectorite (A) before and after pillaring with: (B) ACH, (C) ZACH, and (D) ZCH solutions. Samples were heated in air for 4 h at 400°C.

ings of 6.7 × 7.0 and 2.9 × 5.7 Å, respectively (*14*).

The reaction of commercial hectorite with Al, Al–Zr, and Zr polyoxycations forms pillared clays with Langmuir surface areas of 260–300 m^2/g (stable in air to ~600°C, see Table 2) which after calcination have variable *d*(001) spacing of 16.4, 16.0, and 15.1 Å, respectively. ZCH-hectorite appears to be the most stable structure (Table 2). X-Ray diffractograms showing the clay *d*(001) peak before and after pillaring are shown in Fig. 2. Composition data are shown in Table 1; N_2 pore volume is between 0.14 and 0.18 cm^3/g. If air is replaced by a 95% steam–5% N_2 mixture, between 600 and 650°C the pillared hectorites collapse and the first-order reflection disappears.

The clay catalysts' macroporosity was investigated with Hg intrusion runs at low (0–1200 psig) and high (0–60,000 psig) pressure. Results in Table 3 show that as the pressure increases, Hg intrudes into smaller pores and Hg surface area values in the 25–50 m^2/g range are obtained. In pillared hectorites (and in the parent hectorite) the observed macroporosity is due

TABLE 3

Mercury Porosimetry Data

	P = 1200 psig		*P* = 60,000 psig	
	Surface area, m^2/g	Pore volume, cm^3/g	Surface area, m^2/g	Pore volume, cm^3/g
Hectorite[a]	0.51	0.16	29.4	0.24
ACH-Hectorite	0.34	0.11	39.4	0.17
ZACH-Hectorite	1.85	0.14	36.7	0.25
ZCH-Hectorite	0.39	0.15	49.4	0.21
DL-Hectorite[b]	0.21	0.20	33.7	0.24

[a] Spray-dried sample.
[b] Laponite from Laport Industries.

TABLE 4

Low-Pressure (0–1200 psig) Mercury Porosimetry Measurements

Pore radii (Å)					Volume % in given pore radius range
ACH-Hectorite	ZACH-Hectorite	ZCH-Hectorite	Hectorite[a]	DL-Hectorite	
84,000	95,000	120,000	110,500	500,000	10
38,000	31,500	58,000	68,100	200,000	30
18,300	9,200	27,000	17,000	100,000	50
7,000	19,800	10,500	6,600	56,000	70
2,200	—	2,770	1,850	15,000	90

[a] Spray-dried sample.

mainly to interstices between particles generated by the forming procedure used in preparing the catalysts. In fact, a well-ordered ACH-bentonite catalyst prepared directly from the air-dried clay had a Hg surface area of only ~5 m^2/g at 60,000 psi. In contrast, delaminated clay macroporosity results from edge-to-edge and edge-to-base connections between the synthetic-hectorite (Laponite from Laport Industries) platelets (*15*); 50% of the Hg pore volume thus generated is in pores with radii greater than 100,000 Å (Table 4).

Thermogravimetric (TGA) curves in Fig. 3 show weight losses as a function of temperature. After losing 9% surface water, the natural hectorite weight remains essentially constant up to 550°C. Between 550 and 1100°C dehydroxylation causes an additional 8% weight loss. In contrast, the pillared hectorites weight decreases monotonically with temperature due to losses of water sorbed on the external surface and in the microspace generated by pillaring (Fig. 3). Between 550 and 1100°C there is a 3–5% weight change attributed to removal of water resulting from the crystal lattice dehydroxylation.

After an endotherm between 100 and 200°C (representing water losses), differential thermal analysis (DTA) curves are essentially featureless up to 700°C. Then in the 700–1100°C temperature range, phase transformation occurs (Fig. 4). The major

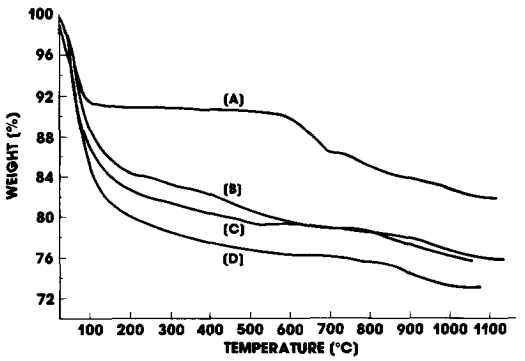

FIG. 3. Thermograms of hectorite (A) before and after pillaring with (B) ACH, (C) ZACH, and (D) ZCH solutions.

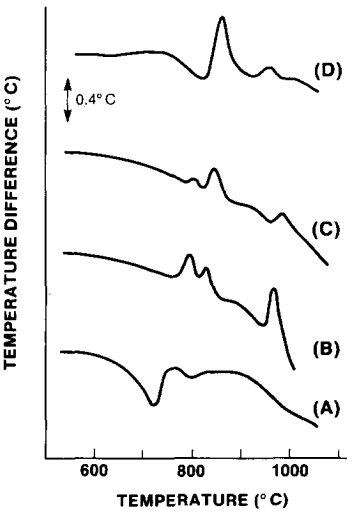

FIG. 4. DTA profiles of hectorite (A) before and after pillaring with (B) ACH, (C) ZACH, and (D) ZCH solutions.

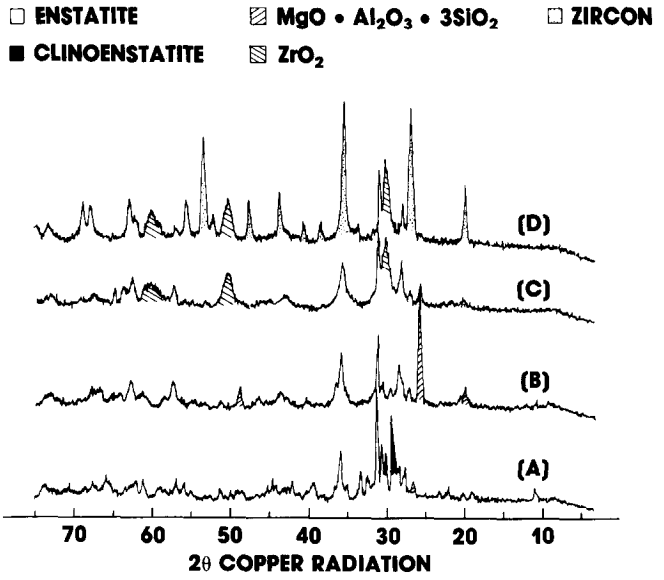

FIG. 5. X-Ray diffractograms of calcined (950°C/h) hectorite before pillaring (A) and after pillaring with (B) ACH, (C) ZACH, and (D) ZCH solutions.

phases formed are identified in Fig. 5. The endotherm at 730°C and the exotherm at 760°C (Fig. 4A) represent the collapse and recrystallization of the parent clay into enstatite ($MgSiO_3$); some quartz is also formed. The broad exotherm at 880°C is attributed to clinoenstatite formation (Fig. 4a). In Fig. 5A, the reflection at $2\theta \cong 10.60°$ is attributed to unreacted dehydrated hectorite. Enstatite (and smaller amounts of clinoenstatite) are also formed by calcining ACH-hectorite at ~800 and 833°C (Figs. 4B and 5B); exotherms between ~970 and 980°C are attributed to magnesium aluminum silicate ($MgO \cdot Al_2O_3 \cdot 3SiO_2$) formation. Between 750 and 850°C (Fig. 4C) ZACH-hectorite forms enstatite and ZrO_2; a small amount of zircon ($ZrSiO_4$) is also formed probably from the interaction of SiO_2 and ZrO_2 (*16*). Zircon is the major phase formed upon calcining ZCH-hectorite in air at 860°C (Fig. 5D); smaller amounts of enstatite an ZrO_2 are also present. The exotherm at ~940°C in Fig. 4D is attributed to a transition from tetragonal to monoclinic ZrO_2. Reference powder data by Brown (*17*) and the 1981 Powder Diffraction File have been used to identify these phases.

Surface Acidity

Spectra for the clay catalysts in the OH stretching region show a prominent free OH band centered between 3650 and 3680 cm^{-1}; a weaker shoulder in the region 3590–3625 cm^{-1} due to H-bonded hydroxyls is seen in all the samples studied (Fig. 6–8). Figure 6E represents the spectra of the acid-washed hectorite before pillaring. After pyridine sorption, only minor changes are observed in the OH region indicating little reaction of these hydroxyl groups with pyridine.

Infrared spectra in the region 1200–1800 cm^{-1} obtained by evacuating the pyridine-containing pillared hectorites at different temperatures are shown in Figs. 9–11. A comparison of these results with those of Parry (*18*) for pyridine on solids indicates that these pillared hectorites, after degassing *in vacuo* (~10^{-6} Torr) at 300°C, contain both Brønsted and Lewis acid sites. In ACH-hectorite, the bands at 1638, 1547, and 1490 cm^{-1}, indicative of pyridinium ion

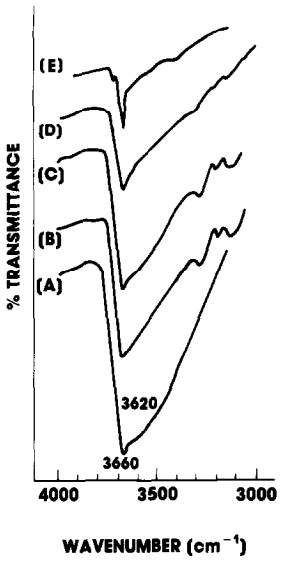

FIG. 6. Hydroxyl absorption bands for ACH-hectorite before (A) and after pyridine sorption and degassing at (B) 200; (C) 300 and (D) 400°C; (E) is the spectrum of the acid-washed and dried-hectorite before pillaring.

formation, decrease in intensity with temperature. At 300°C, the 1638-cm^{-1} band almost disappears; between 300 and 400°C the 1547- and 1490-cm^{-1} bands' intensities are reduced significantly. In contrast,

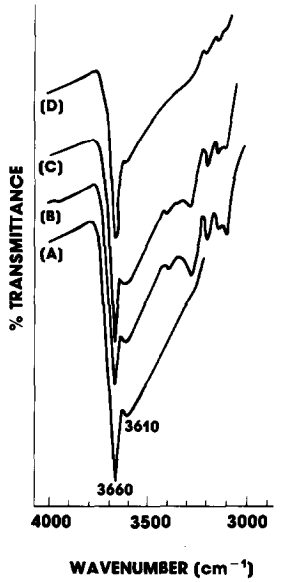

FIG. 7. Hydroxyl absorption bands for ZACH-hectorite before (A) and after pyridine sorption and degassing at: (B) 200, (C) 300, and (D) 400°C.

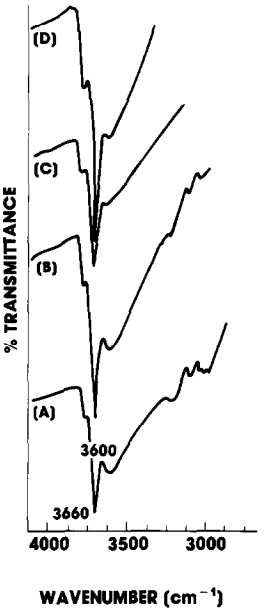

FIG. 8. Hydroxyl absorption bands for ZCH-hectorite before (A) and after pyridine sorption and degassing at: (B) 200, (C) 300, and (D) 400°C.

ZACH- and ZCH-hectorite retain pyridine on Brønsted sites even after degassing at 400°C *in vacuo* (Figs. 10C–11C). Bands in the region 1540–1547 cm^{-1} have been assigned to $>N^{+}—H$ groups, the band at

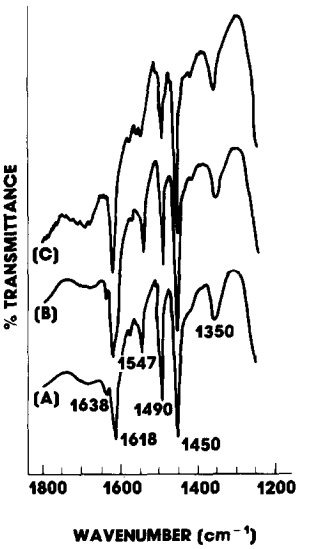

FIG. 9. IR spectra of pyridine sorbed on ACH-hectorite after degassing at: (A) 200, (B) 300, and (C) 400°C.

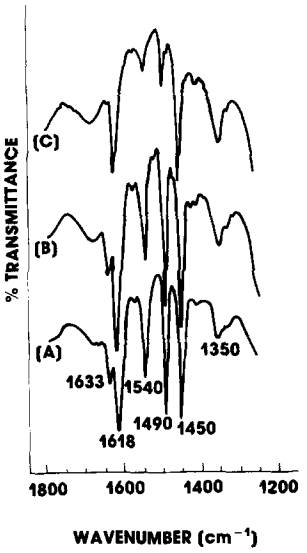

FIG. 10. IR spectra of pyridine sorbed on ZACH-hectorite after degassing at: (A) 200, (B) 300, and (C) 400°C.

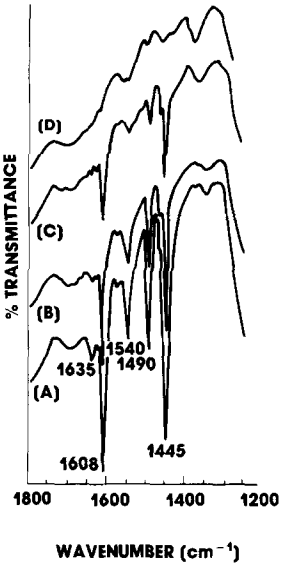

FIG. 11. IR spectra of pyridine sorbed on ZCH-hectorite after degassing at: (A) 200, (B) 300, and (C) 400°C; (D) is the spectra prior to pyridine sorption.

1490 cm^{-1} to pyridine sorbed on both Brønsted and Lewis acid sites (*18*).

Intensities of bands assigned to pyridine coordinated onto Lewis acid sites appear to be almost temperature independent in the 100–400°C range. These are the bands at 1618 and 1450 cm^{-1} in the ACH- and ZACH-hectorite spectra; these bands are shifted to 1608 and 1445 cm^{-1} in ZCH-hectorite. In summary, like bentonites pillared with Al_2O_3 clusters, pillared hectorites (after drying at 300°C *in vacuo*) contain both Brønsted and Lewis acid sites. Above 300°C, *in vacuo*, pyridine is removed first from Brønsted sites and the intensities of its bands at 1547 or 1540 cm^{-1} (and 1490 cm^{-1}) is reduced significantly. In contrast, the intensities of bands assigned to pyridine on Lewis acid sites seem to be temperature independent up to 400°C. The presence of zirconium seems to enhance the pillared hectorite Brønsted acid strength.

After a mild acid-wash with 20% HCl to remove an estimated 15–20% carbonate impurities, the natural hectorite used sorbs pyridine on both Lewis and Brønsted acid sites as indicated by the bands at 1540, 1490, and 1448 cm^{-1}. (In Fig. 12A, the band at 1420 cm^{-1} is attributed to the presence of residual carbonates.) The relative intensities of these bands do not appear to differ significantly from those in Figs. 9–11 indicating that pillaring had little effect on acid

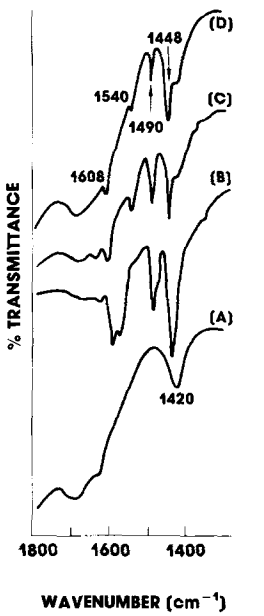

FIG. 12. IR spectra of the acid-washed hectorite before (A) and after pyridine sorption and the degassing at: (B) 200, (C) 300, and (D) 400°C.

sites distribution. As expected, the bands' absolute intensities increase in the pillared hectorites due to a near threefold increase in surface area. The parent (acid-washed) hectorite and the pillared materials have similar acid sites strengths since in both type of catalysts pyridine begins to desorb at ~300°C.

Cracking Properties

Cracking activity for gas oil conversion appears to depend mainly on the surface area generated by ion exchange and dehydroxylation (400°C/4 h) of the polyoxycations used to prop open the silicate layers and not on the pillaring agent used:

	Pillars		
	ZCH	ACH	ZACH
Conversion (*V*% FF, ± 1%)	62.7	64.4	65.2
Langmuir surface area (m^2/g, ± 5%)	298.0	295.0	270.0
BET surface area (m^2/g, ± 5%)	239.0	230.0	201.0
d(001), Å	15.4	16.4	16.0

Before pillaring, the clay had 74.6 m^2/g BET surface area and gave 25.2% conversion. If a zirconyl chloride (ZCH) solution prepared by dissolving 0.25 mol of $ZrOCl_2 \cdot 4H_2O$ in 1 liter of deionized water is used, the pillared product has (after calcination at 400°C/4 h) basal spacing of 16.8 Å and BET surface area of 250 m^2/g. The greater pillar height did not affect the catalyst cracking activity nor product selectivities indicating that cracking reactions also occur outside the pillared structure, that is, in the macropores generated by the forming method used (see Table 3). The ZCH-hectorite with a basal spacing of ~15.1 Å has a Hg surface area of 49.4 m^2/g and partial delamination may have occurred during pillaring.

Pillared hectorites are somewhat less active than corresponding pillared bentonites (*11, 20*). However, liquid products obtained with these type of pillared clays contain greater gasoline fractions. Selectivity does not depend on the pillaring agent used in expanding the silicate layers; the data in Fig. 13 indicate that cut yields (i.e., gasoline; light cycle gas oil, LCGO; and slurry oil, SO) resemble those obtained with a delaminated hectorite (*7*). Higher yields of the valuable LCGO fraction (Fig. 13A) are obtained by cracking more of the heavier components without affecting gasoline production (*11, 19, 20*).

At 67% conversion, the pillared hectorites produced liquids containing 57% gasoline and generated 17% (C_2–C_4). Similarly prepared pillared bentonites gave (at the same conversion level) 49% gasoline and 23% (C_2–C_4). Transition metals impurities are known to catalyze secondary cracking reaction forming light gases (and coke) at the expense of gasoline yields (*21*); the lack of metal contaminants in the parent hectorite is believed responsible for the catalyst's low light gases generation (Figs. 13B and C) and improved gasoline yields.

Carbon generation from these pillared hectorites is similar to that of an iron-contaminated (3–4% Fe_2O_3) pillared bentonite used in cracking gas oil at the same cracking conditions (*11*) (Fig. 13D). The parent hectorite's low iron content (0.3% Fe_2O_3) did not improve the pillared clay's carbon selectivity, indicating that carbon deposits from iron-catalyzed cracking reactions are not the main cause of catalyst deactivation. Hydrocarbon sorption and polycondensation reactions are believed responsible for the pillared clay's high carbonaceous deposits and deactivation (*22*).

CONCLUSION

Pillaring natural hectorite with Al_2O_3, Al_2O_3–ZrO_2, and ZrO_2 clusters generates microporous structures stable in air to 600°C. Initially these clays contain both Brønsted and Lewis acid sites distributed in a manner similar to that observed in the parent (acid-washed) hectorite. Above 300°C *in vacuo*, pyridine is sorbed predominantly on Lewis acid sites. The presence of

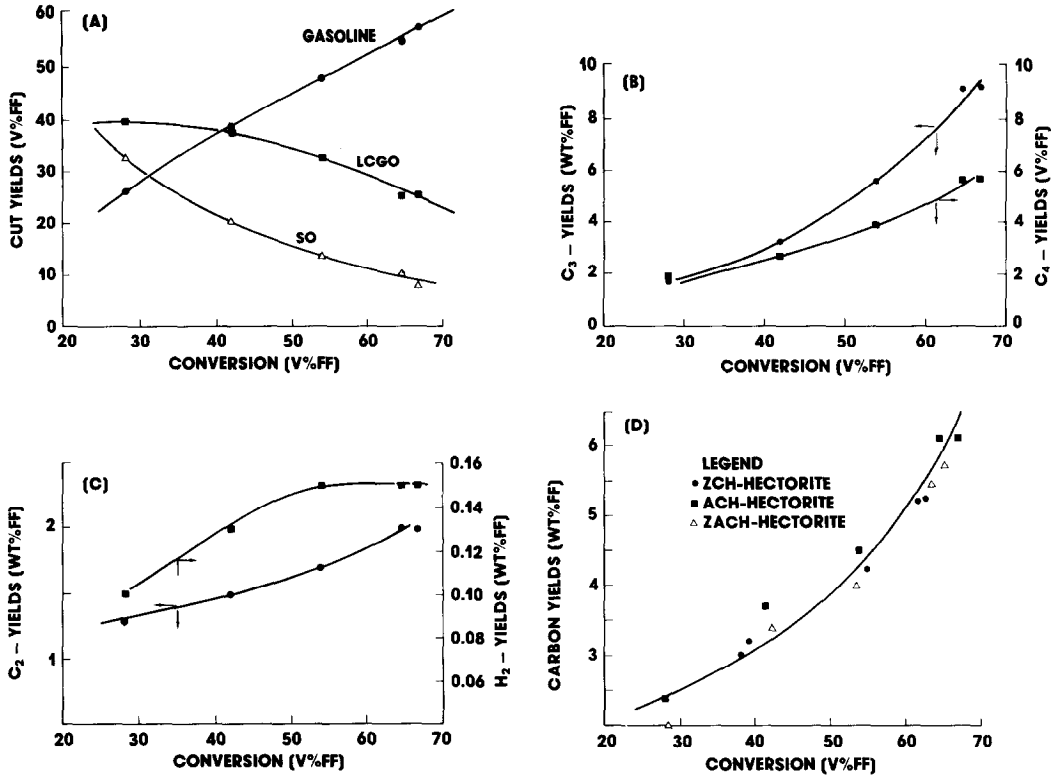

FIG. 13. Product selectivity from gas oil cracking with pillared hectorites: (A) cut yields, (B) C_3 and C_4, (C) C_2 and H_2, and (D) carbon generation.

zirconium enhances the catalyst Brønsted acid strength.

Pillared hectorites exhibit greater gasoline and light gases selectivities but, because of lower surface area, are somewhat less active than the corresponding pillared bentonites in cracking a gas oil at 515°C. Like pillared bentonites, these clay lack the hydrothermal stability of commercially available fluid cracking catalysts containing zeolites.

ACKNOWLEDGMENTS

Special thanks are due to Dr. S. S. Pollack (DOE, Pittsburgh) for many useful suggestions and support during the completion of this work. The assistance received by Ms. Alice Cavanaugh (DOE, Pittsburgh) in obtaining IR data is gratefully acknowledged.

REFERENCES

1. Pinnavaia, T. J., *Science* **220,** 365 (1983).
2. Vaughan, D. E. W., Lussier, R., and Magee, J. S., U.S. Patent 4,176,090.
3. Occelli, M. L., *Ind. Eng. Chem. Prod. Res. Dev.* **22,** 553 (1983).
4. Endo, T., Mortland, M. M., and Pinnavaia, T. J., *Clays Clay Miner.* **28,** 105 (1980).
5. Shabtai, J., Rosell, M., and Tokarz, M., *Clays Clay Miner.* **32,** 99 (1984).
6. Pinnavaia, T. J., Tzou, M. S., Landau, S. D., and Raythathe, R. H., *J. Mol. Catal.* **27,** 195 (1984).
7. Occelli, M. L., Landau, S. D., and Pinnavaia, T. J., *J. Catal.* **90,** 256 (1984).
8. Beckman, S. M., U.S. Patent 2,906,668 (1959).
9. Ciapetta, F. G., and Anderson, D., *Oil Gas J.* **65,** 88 (1969).
10. Yamanaka, S., and Brindley, G. W., *Clays Clay Miner.* **27,** 119 (1979).
11. Occelli, M. L., and Tindwa, R. M., *Clays Clay Miner.* **31,** 22 (1983).
12. Occelli, M. L., Parulekar, V., and Hightower, J. W., *in* "Proceedings, 8th International Congress on Catalysis, Berlin," Vol. IV, p. 725. 1984.
13. Eberly, P. E., *J. Phys. Chem.* **67,** 2404 (1963).
14. Meier, W. M., and Olson, D. H., "Atlas of Zeolite Structure Types." Polycrystal Book Service, Pittsburgh, 1978.
15. Pinnavaia, T. J., *in* "Heterogeneous Catalysis" (B.

L. Shapiro, Ed.), p. 142. Texas A&M Univ. Press, College Station, Texas, 1984.
16. Leverenz, H. W., "An Introduction to Luminescence of Solids." Peter Smith, New York, 1950.
17. Brown, G., *in* "The X-Ray Identification and Crystal Structure of Clay Minerals" (G. Brown, Ed.), p. 467. Mineralogical Society, London, 1961.
18. Parry, E. P., *J. Catal.* **2,** 371 (1963).
19. Lussier, R. J., Magee, J. S., and Vaughan, D. E. W., "Preprints, 7th Canadian Symp. Catal.," p. 102. Edmonton, Alberta, Canada, 1980.
20. Occelli, M. L., *in* "Proceedings, 8th Int. Clay Conf.," Denver, Colorado (1985), in press.
21. Cimbalo, R. N., Foster, R. L., and Wachtel, S. J., *Oil Gas J.* **70** (26), 112 (1972).
22. Occelli, M. L., and Lester, J. E., *Ind. Eng. Chem. Prod. Res. Dev.* **24,** 27 (1985).